EXUDATES DYNAMIC DETECTION IN RETINAL FUNDUS IMAGES BASED ON THE NOISE MAP DISTRIBUTION

Ivo Soares[1], *Miguel Castelo-Branco*[1], *António M. G. Pinheiro*[2]

[1] CICS - Centro de Inv. em Ciências da Saúde, Universidade da Beira Interior, Covilhã, Portugal
[2] Unidade de Detecção Remota, Universidade da Beira Interior, Covilhã, Portugal
Convento de Stº António, 6200-001, Covilhã, Portugal
phone: + (351)75319798, fax: + (351)275319719, email: pinheiro@ubi.pt
www.ubi.pt

ABSTRACT

In this paper a new and reliable method to detect and segment the exudates in retinal fundus images is presented. The introduced approach is based in the computation of the noise map distribution, and on the use of morphological operators and adaptive thresholding. The proposed method reveals a good resilience to contrast changes, non-uniform illumination and variable background, resulting in a correct detection of exudates. A sensitivity of 97.49%, a specificity of 99.95% and an Accuracy of 99.91% is achieved for the exudates detection. Moreover, the method is very effective when applied in the segmentation of the exudates. A comparison is made with recent works. The application of the method shows a strong potential that can be applied in automatic detection and follow-up studies in diabetic retinopathy.

Index terms – Exudates, Noise map distribution, Feature detection, Adaptive threshold.

1. INTRODUCTION

Exudates are one of the most prevalent lesion signs in early diabetic retinopathy, which is the leading cause of blindness. Their detection is of primary importance in early diagnose and follow-ups. Exudates are yellow lipid residues of serous leakage from damaged capillaries, appearing like yellowish lesions, with different shapes and brightness in different locations of the retina [1]. The non-uniform illumination, contrast variation and variable background among different patients are inherent to all retina fundus images. These typical differences are one of main obstacle for good detection of exudates. Shade correction and non-linear point transformation are approaches to overcome non-uniform illumination. However, they need to deal with the difficult discrimination between the variations due to features or illumination [2]. Techniques used in contrast enhancement like histogram equalization or local contrast enhancement face the problems of information loss and noise increment. There are no specific metrics in order to quantify contrast enhancement results, being the final result judge by visual inspection [2].
A considerable number of papers have been published in recent years dealing with the detection of exudates. A complete comparative analysis of the most recent techniques is made on [3]. Contextual information was used with Computer-aided detection systems. The context is based on the spatial relation with surrounding anatomical landmarks and similar lesions [4]. Fuzzy C-means clustering was incorporated with spatial neighbourhood information [5]. Mathematical morphologic methods have been used [6,7]. Neural Networks and Support-vector machines were used in [8]. Split-and-merge techniques, where region candidates are detected using a combination of coarse and fine segmentation were used in [9]. An approach based on Fisher's linear discriminant analysis making use of color information was introduced in [10]. Naive Bayes and Support Vector Machines classifiers were employed in [11].
Noise is an unwanted characteristic inherent to all retina images resulting from stochastic fluctuations. The normal approach is to remove or reduce it [4]. It does not come associated with techniques specially designed to perform segmentation of exudates. In this work a technique that is highly resilient to contrast variations and non-uniform illumination is proposed. It is based on the computation of the noise map distribution and the use of morphological operators. A binary image representative of the original retinal fundus that can be easily interpreted is generated. This binary image, called Regional Maxima Noise Distribution Function (I_{ndf}) is used to perform the detection of the exudates using concentric binary masks and automatic adaptive threshold. The detection of exudates is achieved without any preprocessing. That shows the robustness of the method for exudates detection and segmentation on images with non-uniform illumination. The DIARETDB1 [12] data base with 89 color retinal fundus images with a 1500x1152 size was used for testing and performance evaluation. The optic disk was manually removed from all the images, because this feature has chromatic and intensity signatures similar to the exudates. Ground truth masks are provided for all images in the database.

2. REGIONAL MAXIMA NOISE DISTRIBUTION COMPUTATION

For the exudates detection we make use of the green component of the RGB image I_G, since it is the component that

offers larger contrast [4]. I_G, may be interpreted as the composition,

$$I_G = I_F + I_B \quad (1)$$

where I_F is the foreground image and I_B is the background image [13]. Features like the optic disk, vasculature branches, and any visible lesion belong to the I_F image. The background image I_B, contains all the illumination variation due to the acquisition transformation function, and is the ideal image of the retina without any feature [2]. I_B can be statistically modeled as

$$I_B \sim N(\mu, \sigma) \quad (2)$$

i.e., as a white and random field with mean value μ, that represents the ideal uniform luminosity value, and standard deviation σ, that represents the natural variability of retinal fundus pigmentation. Furthermore, sub-regions in I_B also obey a normal distribution [13]. To separate exudates from the background and low intensity features, the I_G image is considered as a topographic map where peaks and valleys correspond respectively to high and low intensity pixels. Since exudates are regions with high intensity pixels a regional maximum detection technique is employed. A neighborhood of dimension $5x5$ and centered in an arbitrary pixel p, W_5 is considered. The size of the neighborhood was selected based on experimenting tests. For all the pixels p belonging to the image I_G, the regional maxima of the image I_G is determined with the following condition,

$$if\ I_G(p) \geq I_G(p)_{W_5} \Longrightarrow I_{ndf}(p) = 1,$$
$$else\ I_{ndf}(p) = 0 \quad (3)$$

where I_{ndf} is a binary image that represents the regional maxima of the noise map distribution of image I_G. Equation (3) can produce the detection of pixels or regions of maxima [14]. The regions of maxima are replaced by the pixel with the higher intensity value in each region Fig.1 b). Although noise affects the entire image I_G, certain patterns in the noise distribution can be noticed by analyzing I_{ndf}. There are areas with a denser and uniform distribution of points and areas with a sparse and irregular distribution. The noise effect is more noticeable in the background regions of I_G, where the pixels have small variation of the color components between neighbor pixels. Because of that, Equation (3) produces a dense and uniform distribution of points in those background regions. In opposition, features like exudates and vascular branches represent areas of I_G where the pixels intensities values vary more abruptly and the noise effects are not so noticeable. Features will then belong to sparse and irregular regions in I_{ndf}. Equation (3) only searches for regional maximum, meaning that only peaks will be selected and marked, in opposition to the valleys points. Features with low intensity values like vascular branches and hemorrhages will not result in valley points marked in I_{ndf}. Exceptions can occur in arteries where the central zones can have brighter pixels (Fig.1 d)). Features

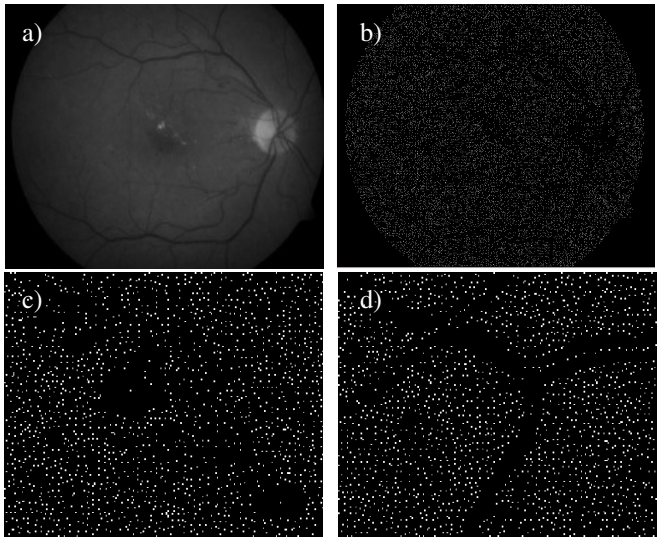

Figure 1 - Upper images: a) represents an fundus image and b) I_{ndf}. Lower images: c) exudates and d) vasculature samples in I_{ndf}.

with high intensity pixel values like exudates belong to sparse and irregular regions. The effect of noise is not so noticeable due to the intensity growing towards the exudate centre. Hence, in such areas only one or a small number of pixels are marked (Fig.1 c)). These characteristics enable the separation of exudates from background, resulting in their detection and segmentation. The optic disk is a feature that shares same common characteristic and it is manually removed from all the images before exudates segmentation. Although resulting from a simple condition (equation (3)), I_{ndf} is very resilient to contrast changes, and non-uniform illumination, retaining the limit pixels, shape characteristics and the peak pixels of the exudates, independently of their location.

3. EXUDATES SEGMENTATION

To perform the exudates segmentation a region-processing solution is adopted. In each region an analysis of the intensities pixels of I_G that are also marked in I_{ndf}, is performed using dynamic thresholding. In the usual approach square regions with different sizes are considered [9]. In this work the regions are defined following a different approach. The shapes of the regions are chosen taking into account the oblate cup shape of the retina and that the retinal image acquisition has an approximately spherical illumination distribution pattern. Anatomically, the retina can be modeled as an oblate cup shape, where the macula is the pole. Most of the retina images are acquired with the macula in the centre or near the centre, since the patient is instructed to look towards a fixation central point. This ensures the alignment of the macula with the fixation point of the fundus camera. Hence it is assured that the macula will be in a central region of the retinal image. Although it can be affected by defocus, opacities and by the acquisition with

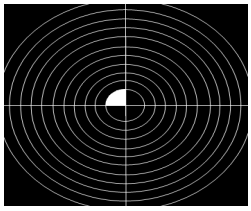

a) Binary mask D

b) Region D_1

Figure 2 - Region model

different fundus cameras, the approximately spherical illumination distribution pattern, result in lighter central areas than the peripheral areas. Consequently, different levels of contrast appear across the retina image. This must be considered for the definition of the segmentation regions. A black-and-white mask BW, where white represents retina information and black does not have any information is defined for the retina image. The dimensions of BW, defines the limits of the regions. These limits are dynamically computed, according to a binary mask D, centered in BW and formed by concentric quarter rings equally spaced, as shown in Fig. 2 a). Each quarter of the ring delimits the regions where the segmentations will be performed. Fig. 2 b) shows the first binary region, D_1 constructed according to D. N_D is the total number of regions D_i. Another advantage with this region model, is that although D may not be centered with the macula, it will be very close to it. Since the central regions in D are smaller than the peripheral ones, a more precise macular analysis is performed. For each mask D_i , $(i = 1\ to\ N_D)$, M_i is defined as,

$$M_i = \left(D_i \cap I_{ndf}\right) o\, I_G\ ,\ (i = 1\ to\ N_D) \tag{4}$$

where o is the Hadamard product. The result is a set of N_D images M_i, with the intensity pixels selected by the equation (4). After selecting these intensity pixels for each M_i, it is possible to construct a set of N_D vectors $V_i(x)$, where x represents the selected pixels inside M_i. $V_i(x)$ can be interpreted as the sampling of the intensities pixels belonging to I_G and to I_{ndf} for each region D_i. The process is illustrated in Fig. 3 a) for $V_1(x)$. The pixels in $V_i(x)$ can represent two different situations. They are pure background pixels if they are selected in regions where no features exist. In that case they can be statistically modeled as a normal distribution, according to equation (2). Otherwise they are a region with exudates or other feature with high intensity pixels. In this case, they cannot be approximated by a normal distribution. However, in both situations the values $V_i(x)$ plotted in ascending order result in similar plots to the ones represented in Fig.3 b). The plots show the existence of a point where $V_i(x)$ bends more sharply. This point is called the critical intensity value c_i. Every vector $V_i(x)$ represented in ascending order results in a critical intensity value. This c_i value is used to segment the exudates areas from the background in each region D_i. The computation of c_i is explained in the next section. To perform the exudates segmentation we select all the points in each region mask D_i that simultaneously belong to the I_G

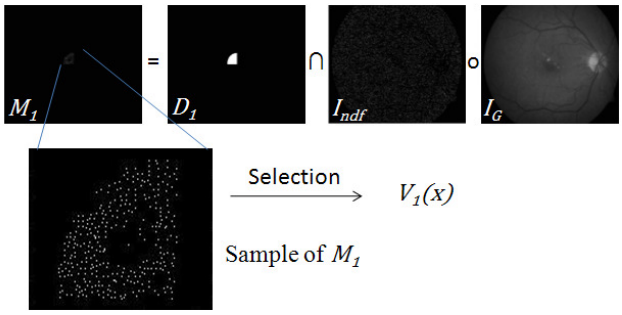

a) Example of $V_1(x)$ computation.

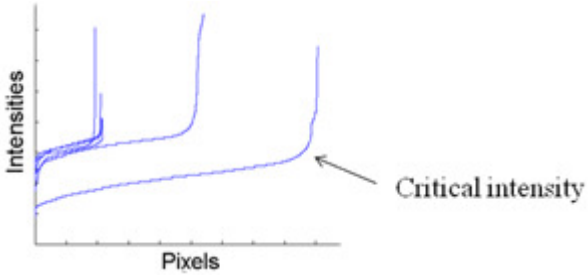

b) Plotted intensities in ascending order of some $V_i(x)$

Figure 3 - $V_i(x)$ computation

image, and have an intensity value larger than the corresponding c_i. For every pixel p belonging to the I_G image and to the region D_i,

$$if\ I_G(p)_{D_i} > c_i \rightarrow S_i(p) = 1\ ,(i = 1\ to\ N_D)$$
$$else\ S_i(p) = 0 \tag{5}$$

The process is repeated in each region D_i . The final segmentation image S, is obtained with the union of the N_D segmented regions S_i,

$$S = \bigcup_i^{N_D} S_i \tag{6}$$

The method reveals to be very effective in regions where exudates exist. The problem arises in regions without exudates. The calculation of c_i in these regions implicates the appearance of artifacts, erroneous regions marked as exudates. To perform the selection between artifacts or exudates an algorithm based in the noise distribution I_{ndf} is presented in section 3.2.

3.1 Critical intensity determination

The critical intensity c_i must be computed with the best possible accuracy. If it is too large, points that may belong to exudates may not be selected, resulting in under-detection. If it is too small, exceeding points will be selected, resulting in over-detection. In order to improve the detection of c_i a polynomial interpolation of $V_i(x)$ was performed and $F_i(x)$ was computed according to,

$$F_i(x) = \frac{d\,V_i(x)}{dx} \tag{7}$$

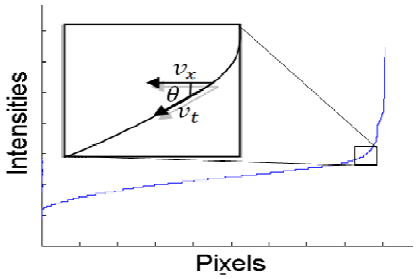

Figure 4 – Critical intensity calculation.

Fig. 4 represents $F_i(x)$for any given region D_i. The derivative results in a stronger bending of $F_i(x)$ leading to a more accurate computation of the threshold value. Considering an angle θ between the tangent vector in $x, \boldsymbol{v_t}$, and the horizontal vector $\boldsymbol{v_x}$, as show in Fig. 4. The critical intensity will be the point in which the angle θ, between the vectors $\boldsymbol{v_t}$ and $\boldsymbol{v_x}$ reaches 45^o. Starting from the last position in $F_i\,(x)$, the angle θ is calculated for every point x until it reaches 45^o. The first position x with $\theta = 45^o$, is selected as the critical intensity. The c_i values calculated with this procedure are used in equation (4).

3.2 Artifacts removal

As referred earlier, it is impossible to avoid the appearance of artifacts. When c_i is computed for an image region without exudates it is likely the appearance of some segmented areas, and hence they will be incorrectly marked. These artifacts are removed using a selection process based in the dispersion of I_{ndf}, and the segmented regions marked in S. A labeling of the white areas in S is performed - A_l. In order to classify A_l as exudate or artifact, the algorithm of Fig. 5 is used. The algorithm analyses the A_l pixels and their position in I_{ndf}. Pixels located in the proximity of high density regions are deleted. In the opposite case they are preserved. FA_l represents the percentage of suppressed pixels that each A_l suffers after the selection process is complete. The best performance was achieved for a FA_l value of 12 (similar FA_l values result in identical results). This means that A_l areas that suffers a pixels suppression larger than 12% after the selection process will not be considered as exudates, and are removed from the segmentation. A_l areas that represent true exudates, belong to regions of I_{ndf} with low density pixels, resulting in almost no pixel suppression. Hence, those areas are preserved as segmented areas. Fig. 7 shows the final segmentation result for an image that belongs to the images database.

Consider a binary circular mask AC, $radius = 4$, with dimension $9x9$. For each labeled region, A_l,

1. Count the total number of white pixels, N_o in A_l,

$$N_o = Card(A_l)$$

1.1 For each pixel p, belonging to A_l, consider the neighborhood of p with dimension $9x9$, W_9 in I_{ndf}. Compute,

$$k = Card(I_{ndf}\,(p)_{W_9} \cap AC)$$

$$if\ k < 2\ then, delete\ p\ from\ A_l$$

2. Compute

$$N_f = Card(A_l)$$

$$if(100\text{x}N_f)\ /\ N_o > FA_l\ then,$$

$$S(p)_{p\in A_l} = 0$$

Figure 5 - Artifacts removing algorithm

4. RESULTS AND DISCUSSION

The DIARETDB1 [5] data base with 89 color retinal fundus images with size 1500x1152 was used for testing and performance evaluation. Ground truth masks are provided for all images in the database. 46 of these images contain exudates while 43 are normal or contain other type of lesion. The provided ground truth images are the result of several markings made by different experts for each retinal fundus image. Depending of the number of experts marking the different areas, different confidence levels can be defined. The performance of the proposed algorithm was tested and evaluated, comparing the results with the ground truth images at a pixel level. This evaluation results in the computation of the Sensitivity, Specificity and Accuracy. To test this method a set of 28 training images defined in DIARETDB1 (19 with exudates and 9 normal or with other type of lesion) were used. The method depends in the following parameters; N_{ring} - number of rings used to create D, FA_l - the pixels suppression factor, Ic_i – incrementing interval for each c_i, constant k, W_9 and W_5. These parameters were tested in the following variations intervals, $N_{ring} \in \{2{:}\,15\}$, $FA_l \in \{8{:}\,30\}$, $Ic_i \in \{-10{:}\,10\}$, $k \in \{1,2,3,4\}$ and W_9, W_5, $AC \in \{3x3, 5x5, 9x9, 11x11\}$. After testing the different combinations, the highest sensitivity and specificity results for $N_{ring} = 9$, $FA_l = 12$, $Ic_i = 0$, $W_9 = 9x9$, $W_5 = 5x5$, $AC = 9x9$ and $k = 2$. Using these parameter values, a performance evaluation of the described method was done using the evaluation set of the 61 remaining images defined in DIARETDB1 (28 with exudates and 33 normal or with other lesion). The best sensitivity, specificity and accuracy are 97.49% , 99.95% and 99.91% respectively with a confidence level of 0.7, computed at pixel level (only detected pixels are considered for performance evaluation). The ROC plot for our algorithm was achieved considering the best parameters values and different confidence levels, showing a normalized area under the curve of 96.89% (Fig. 6). Moreover, the images with no exudates result in a mean error of 0.004% marked regions. This is a critical situation, because images with no exudates tend to create spurious segmented regions, due to the dynamic thresholding. Table 1 shows a comparison of this method performance (for a confidence level of 0.7) with some of the most recent methods.

5. FINAL COMENTS

A method that performs a correct detection and segmentation of exudates in retinal images was developed. The defined I_{ndf} image is resilient to contrast changes and non-uniform illumination, resulting in a very accurate detection. The selection of the critical intensity locally, results in an accurate dynamic thresholding computation. This is concluded because when the computed dynamic threshold was changed in

Reference (using DIARETDB1)	Se %	Sp %	Acc %	NI
Our Method	97.49	99.95	99.91	61
Kande [5]	86	98	-----	47
Welfer [6]	70.48	98.84	-----	47
Jaafar [9]	89.3	99.3	99.4	47
(using other database)				
Sopharak[11]	92.28	98.52	98.41	39
Garcia [8]	88.14	92.6	97	67
Ravishankar[7]	94.16	91.1	------	516

Table 1 - Comparison of exudates detection methods.
Se -Sensitivity, Sp - Specificity, Acc – Accuracy,
NI- Number of images.

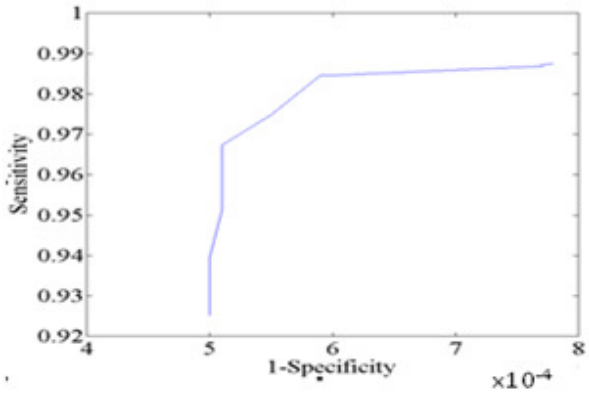

Figure 6 - ROC plot for the best parameters values and different confidence levels.

the interval $Ic_i \in \{-10{:}\,10\}$, the value of $Ic_i = 0$ leaded to the best result. This means that the computation of the Critical Intensity Value is accurate and does not need any correction. The concentric regions dynamically defined to every fundus image, proved to be very effective in the segmentation task. Unfortunately the ground truth regions are not accurate and in some cases they join two different exudates in one region (as noted in [15]). In those cases, the validation of the detection results is impossible (if only one of those exudates is detected, there is no possibility of quantifying that error). Although uncommon, that situation can produce a slight decrease in the Sensitivity results of figure 6 and table 1. Moreover, this is a common situation to other results obtained with this database. In [15] is described an attempt to avoid this situation without accurate results. Because of this, the evaluation of the segmentation accuracy is an important issue that requires future consideration. The effective detection and delimitation of the optic disk using the shape preservation that I_{ndf} provides will be studied in the future. The authors would like to thank the DIARETDB1 database creators.

6. REFERENCES

[1] G. B. Kande, P. V. Subbaiah, T. S. Savithri, "Feature extraction in digital fundus images," Journal of Medical and Biological Engineering, vol. 29, No. 3, 2009.

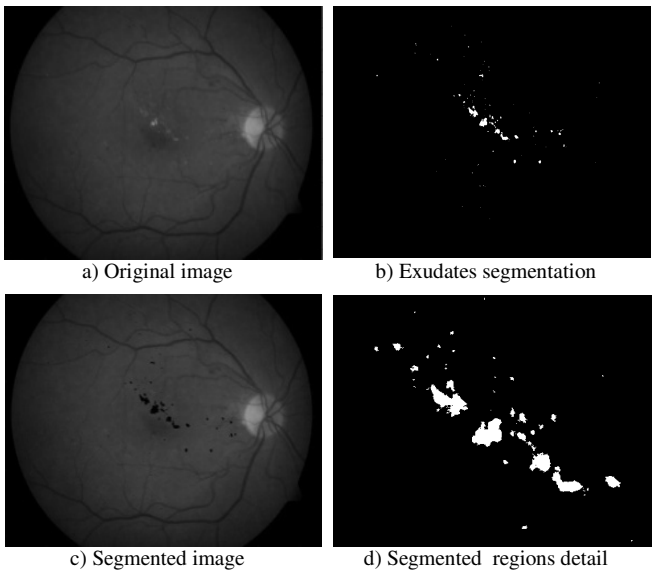

a) Original image b) Exudates segmentation

c) Segmented image d) Segmented regions detail

Figure 7 - Example of exudates segmentation with the proposed algorithm.

[2] R.J. Winder et al., "Algorithms for digital image processing in diabetic retinopathy," Computerized Medical Imaging and Graphics, vol. 33, pp. 608-622, 2009.
[3] A. Sopharak, B. Uyyanonvara, S. Barman T. Williamson,"Comparative Analysis of Automatic Exudate Detection Algorithms", WCE, London, Vol. I, 2010.
[4] C. I. Sánchez et al., "Improving hard exudates detection in retinal images through a combination of local and contextual information", ISBI, pp 5-8, 2010.
[5] G. Kande, P. Subbaiah and T. Savithri, "Segmentation of Exudates and Optic Disk in Retinal Images", IEEE 6th Indian Conf. on Computer Vision, Graphic & Image Processing, 2008.
[6] D. Welfer, et al., "A coarse-to-fine strategy for automatically detecting exudates in color eye fundus images", CMIG, 2009.
[7] S. Ravishankar, A. Jain, A. Mittal, "Automated Feature Extraction for Early Detection of Diabetic Retinopathy in Fundus Images", CVPR, 2009.
[8] M. Garcia et al., "Neural network based detección of hard exudates in retinal images", Computer Methods and Programs in Biomedicine, vol. 93, pp. 9-19, 2009.
[9] H. Jaafar, A. Nandi, W. Al-Nuaimy, "Automated Detection of Exudates in Retinal Images Using a Split and Merge algorithm", EUSIPCO, 2010.
[10] C. I. Sanchez et al., "A novel automatic image processing algorithm for detection of hard exudates based on retinal image analysis", Medical Engineering & Physics, vol. 30, pp. 350–357, 2008.
[11] A. Sopharak et al., "Machine learning approach to automatic exudate detection in retinal images from diabetic retinopathy", Journal of Modern Optics, pp. 1-12, 2009.
[12] T. Kauppi et al., "DIARETDB1 diabetic retinopathy database and evaluation protocol, " Proc of the 11th Conf. on Medical Image Understanding and Analysis, 2007.
[13] M. Foracchia , E. Grisan, A. Ruggeri, "Luminosity and contrast normalization in retinal images", Medical Image Analysis, vol. 9, pp. 179–190, 2005.
[14] Z. B. Sbeh, L. D. Cohen, "A New Approach of Geodesic Reconstruction for Drusen Segmentation in Eye Fundus Images", IEEE Trans. on Medical Imaging, vol. 20, no. 12, December, 2001.
[15] K. Ram, J. Sivaswamy, "Multi-space clustering for segmentation of exudates in retinal color photographs", EMBC, September, 2009.